Computational and Structural Biotechnology Journal 18 (2020) 2610–2620

COMPUTATIONAL AND STRUCTURAL BIOTECHNOLOGY JOURNAL

journal homepage: www.elsevier.com/locate/csbj

Exploration of gastric neuroendocrine carcinoma (GNEC) specific signaling pathways involved in chemoresistance via transcriptome and *in vitro* analysis

Jianwei Xie [a,1], Pengchen Chen [b,1], Hongteng Xie [a,1], Yuqin Sun [a,e], Zhen Huang [c], Ran Wei [b], Zhengqiang Miao [b], Qingshui Wang [c], Shu-Dong Zhang [d], Koon Ho Wong [b], Yao Lin [c,f,*], Changming Huang [a,*], Hang Fai Kwok [b,*]

[a] *Department of Gastric Surgery, Fujian Medical University Union Hospital, Fuzhou, Fujian 350000, PR China*
[b] *Cancer Centre, Faculty of Health Sciences, University of Macau, Avenida da Universidade, Taipa, Macau SAR*
[c] *College of Life Sciences, Fujian Normal University, Fuzhou, Fujian 350000, PR China*
[d] *Northern Ireland Centre for Stratified Medicine, Biomedical Sciences Research Institute, Ulster University, Londonderry BT47, United Kingdom*
[e] *Department of General Surgery, Zhangzhou Affiliated Hospital of Fujian Medical University, Zhangzhou 363000, PR China*
[f] *Key Laboratory of OptoElectronic Science and Technology for Medicine of Ministry of Education, Fujian Normal University, Fuzhou, Fujian 350000, PR China*

ARTICLE INFO

Article history:
Received 23 July 2020
Received in revised form 8 September 2020
Accepted 10 September 2020
Available online 20 September 2020

Keywords:
Transcriptome analysis
GNEC
GAC
NeuroD1
Chemoresistance

ABSTRACT

Gastric neuroendocrine carcinoma (GNEC) is rare cancer detected in the stomach. Previously, we demonstrated that the poorer prognosis of GNEC patients compared with gastric adenocarcinoma (GAC) patients was probably due to the lack of response to chemotherapy. Thus, it is crucial to study the specific GNEC gene expression pattern and investigate chemoresistance mechanism of GNEC. The transcriptome of GNEC patients was compared with that of GAC patients using RNA-seq. The KEGG analysis was employed to explore the specific differential expression gene function enrichment pattern. In addition, the transcriptomes of two GNEC cell lines, ECC10 and ECC12, were also compared with those of two GAC cell lines, MGC-803 and AGS, using RNA-seq. Comparing patient samples and cell lines transcriptome data, we try to uncover the potential targets and pathways which may affect the chemoresistance of GNEC. By combing all transcriptome data, we identified 22 key genes that were specifically up-regulated in GNEC. This panel of genes probably involves in the chemoresistance of GNEC. From our current experimental data, NeuroD1, one of the 22 genes, is associated with the prognosis of GNEC patients. Knockdown of NeuroD1 enhanced the sensitivity to irinotecan of GNEC cell lines. Our research sheds light in identifying a panel of novel therapeutic target specifically for GNEC clinical treatment which has not been reported before.

1. Introduction

Gastric neuroendocrine carcinoma (GNEC) is a rare cancer found in the stomach and accounts for about 4.1% of all neuroendocrine tumors [1]. According to "Trends in the Incidence, Prevalence, and Survival Outcomes in Patients with Neuroendocrine Tumors in the United States" and "Epidemiological trends of pancreatic and gastrointestinal neuroendocrine tumors in Japan", the incidence of GNEC is increasing in America [2,3]and Japan [4]. The malignancy and prognosis of GNEC are significantly different from gastric adenocarcinoma (GAC) [5] and most GNEC display more malignant behaviors [1]. However, little is known about the typical clinical manifestations or biological and pathological characteristics of GNEC. Currently, two neuroendocrine tumor makers, CgA (chromogranin A) and SYN (synapsin) are employed for the diagnosis of GNEC in pathology. In recent years, the treatment of GNEC has reached an agreement, and it is generally believed that surgical resection is the most effective treatment for this disease

* Corresponding authors at: Department of Gastric Surgery, Fujian Medical University Union Hospital, Fuzhou, Fujian 350000, PR China (C. Huang); College of Life Sciences, Fujian Normal University, Fuzhou, Fujian 350000, PR China (Y. Lin); Cancer Centre, Faculty of Health Sciences, University of Macau, Avenida da Universidade, Taipa, Macau SAR (H. F. Kwok).

E-mail addresses: yaolin@fjnu.edu.cn (Y. Lin), hcmlr2002@163.com (C. Huang), hfkwok@um.edu.mo (H.F. Kwok).

[1] Authors contributed equally to this work.

https://doi.org/10.1016/j.csbj.2020.09.016

[6,7]. TNM staging and lymphocyte ratio were reported to predict the prognosis of GNEC and the levels of CgA and gastrin found to be danger factors of GNEC in early diagnosis [8–10]. However, these studies cannot explain the pathogenesis of GNEC. In China, GNEC patients are often treated as GAC patients with similar chemotherapeutic drugs including fluorouracil, cisplatin, streptomycin, allium annulus and paclitaxel [11,12]. In our previous study, we reported that the poorer prognosis of GNEC patients compared with GAC patients is probably due to the lack of response to chemotherapy [13]. Therefore, it is important to optimize the chemotherapy strategy for GNEC treatment. For example, netazepide was reported to slow down GNEC tumor growth and somatostatin analogue found to have better effect on functional GNEC but not nonfunctional GNEC [14]. However, so far there have no studies on the molecular characteristics of GNEC, which will provide critical insight for developing and identifying more specific therapeutic targets and more effective chemotherapy strategies.

2. Materials and methods

2.1. Cell culture

GNEC cell lines ECC10 and ECC12 were purchased from RIKEN BRC CELL BANK (Japan). Similar to GAC cell line NUGC, MKN74, MKN45, KATO III, HGC and MGC-803, GNEC cell line ECC10 and ECC12 were cultured in RPMI 1640 supplemented with 10% fetal bovine serum (FBS) while AGS was cultured in DMEM/F12 supplemented with 10% FBS (Thermo Scientific). Cells were kept at 37 °C in a humidified incubator with 5% CO2.

2.2. Human specimens for RNA-seq

The resected carcinoma and paired adjacent tissue specimens of patients were stored in liquid nitrogen, and a fraction of each was sent for pathology inspection to confirm the diagnosis. The details of patient information were listed in Table 1. The study was approved by the ethics committee of Fujian Medical University Union Hospital (Fujian, China; 2017KY090). Human tissue specimens collected for this study were from residual tissue in blocks generated for gastrectomy processing. All patients signed informed consents agreeing on further examinations and investigations. The tissue specimens were stored in TRIZOL (Invitrogen) and sent to Sangon Biotech (Shanghai) Co., Ltd for sequencing.

2.3. Immunohistochemistry (IHC)

Tumor specimens of 50 GNEC patient were obtained from Fujian Medical University Union Hospital (Fujian, China) with detailed clinic pathologic parameters. All patients underwent gastrectomy between 2008 and 2013. The detailed protocol of IHC staining was followed as previously described. Rabbit anti-human NeuroD1 antibody was purchased from Proteintech. The IHC-stained tissue sections were reviewed under a microscope by two pathologists who were blinded to the clinical parameters and scored independently according to the intensity of cellular staining and the proportion of stained tumor cells. In cases of discrepancy, we re-evaluated the samples and consensus scores were chosen for evaluation. The staining intensity was scored as 0 (no staining), 1 (weak staining, light yellow), 2 (moderate staining, yellow–brown) and 3 (intense staining, brown). The proportion of stained tumor cells was classified as 0 ($\leq$5% positive cells), 1 (6% to 25% positive cells), 2 (26% to 50% positive cells) and 3 ($\geq$51% positive cells). The NeuroD1 protein expression was considered low if the total score (distribution score + intensity score) was 3 or less and high if 4 or more.

2.4. mRNA extraction, RNA-Seq and data analysis

Total RNAs were extracted from tissues and cell samples using Total RNA Extractor (Trizol) Kit (Sangon Biotech) following the manufacturer's instructions for further RNA-Sequencing. The integrity and quality of total RNAs were assessed by 1% (w/v) agarose gel electrophoresis and the 260 nm/280 nm absorbance ratio using a NanoDrop® ND-1000 spectrophotometer. Briefly, mRNA was gathered using magnetic beads with oligo (dT) and then fragmented into short fragments, which were prepared as templates to synthesize the cDNA library. Sequencing of cDNA library was carried out on Illumina Hiseq™ using the paired-end technology. Reads were mapped aligned to the genome assembly Homo sapiens. GRCh38 using HISAT2 and proceeded statistics by RSeQC. The TPM values were calculated for each transcript using StringTie. Differentially expressed genes (DEGs) were evaluated by taking 2-fold changes, $p < 0.05$ and $q < 0.05$ as criteria. Further, Gene Ontology (GO) enrichment analysis and Kyoto Encyclopedia of Genes and Genomes (KEGG) pathway enrichment analyses were performed using DAVID bioinformatics resources 6.8 (https://david.ncifcrf.gov/).

2.5. Quantitative reverse transcription PCR (qRT-PCR)

Total RNA extraction from cell lines and qRT-PCR procedure followed as previously described [15].GAPDH was used as a loading control. The primer sequences can be found in Appendix Table S1.

2.6. Establishment of stable cell lines

Lentiviral constructs of NeuroD1-overexpression, NeuroD1-shRNA and their matched empty vectors were purchased from Obio Technology (Shanghai) Corp., Ltd. Cells were seeded in 6-well plate at the concentration of 105 cells per well before lentivirus infection. Once the confluence of cells reached around 30%, cells were infected with the lentiviruses at a suitable multiplicity using polybrene (10 mg/ml). The cell state was observed after 6–8 h and the culture media were replaced with fresh media. After culturing for 48 h, the cells were selected with the corresponding antibiotic puromycin (Sigma). Finally, the cells were harvested for mRNA and protein analysis to verify the establishment of stable cells before expansion.

2.7. Cell proliferation detection

According to different growth characteristics of the cells, ECC10 and ECC12 were planked at a density of 104 cells/well in 96-well plates while AGS and MGC-803 at a density of 10^3 cells/well. After 24 h, cells were respectively exposed to gradient concentrations of 5-fluorouracil, cisplatin, irinotecan and oxaliplatin (Sigma-Aldrich). Cells were sequentially cultivated for 72 h. The cell viability was detected using Cell Counting Kit 8 (TransGen Biotech) following the manufacturer's instructions. The cell proliferation was detected by Sulforhodamine B (Sigma-Aldrich) as previously described [16].

2.8. Western blot

Total cellular proteins were extracted in RIPA lysis buffer and centrifuged at 16,000g, 4 °C for 15 min. The protein concentration was quantified using the BCA kit (Thermo Scientific). Equal amounts of protein sample were separated on 12% SDS-PAGE gels and then transferred to nitrocellulose membrane. Membranes were blocked in 5% skim milk in PBS for 1 h at room temperature, incubated with primary antibody (anti-NeuoD1, Proteintech 12081-1-AP and anti-actin, Abcam ab115777) overnight at 4 °C and subsequently with its respective secondary antibody at room

Table 1
Characteristics of patients.

Patient ID	Age	Sex	pathology type	Tumor stage
T1	65	Male	MANEC (40% for large cell type, 60% for adenoacrcinoma)	pT3N1M0
T2	60	Female	NEC (large cell type)	pT3N3M0
T3	75	Female	NEC (90% for small cell type, 10% for large cell type)	pT3N2M0
T6	65	Male	adenocarcinoma (moderately differentiated)	pT3N1M0
T7	58	Female	adenocarcinoma (poorly differentiated)	pT3N3M0
T8	74	Female	adenocarcinoma (poorly differentiated)	pT3N2M0

MANEC: mixed adenoneuroendocrine carcinoma.
NEC: neuroendocrine carcinoma.

temperature for 1 h. The binding signals were quantified using Odyssey (LI-COR).

3. Results

3.1. Transcriptome analysis of the gastric neuroendocrine tumor tissue

RNA-seq analysis was performed using three pairs of GNEC patient samples that covered all pathological features, including one pair of mixed adenoneuroendocrine carcinoma (MANEC) that was intermingled with areas of squamous cell carcinoma or adenocarcinoma, each comprising at least 30% of the tumors. An additional RNA-seq analysis was also performed using three pairs of matched GAC patient samples to help identify GNEC-specific gene expression (Table 1). Through tissue transcriptome pattern distance and cluster analysis, we noticed that the GNEC patient tumor tissue samples (GN-T1, GN-T2 and GN-T3) were more similar to each other compared with other tissue samples (Fig. 1B) including GNEC non-tumor tissues (GN-N), GAC tumor tissues (GA-T) and GAC non-tumor tissues (GA-N) (Fig. 1A), suggesting the existence of GNEC specific gene expression panel. In summary, 3295 genes were up-regulated, and 151 genes downregulated in the GNEC tumor samples compared with their adjacent non-tumor tissues (Fig. 1B). In the three pairs of GAC patient samples, 7346 genes were up-regulated, and 144 genes downregulated in the GAC tumor samples compared with their adjacent non-tumor tissues (Fig. 1C). Further KEGG analysis indicated the specific up-regulated genes in GNEC patient samples were mainly enriched in the following pathways: cell cycle, maturity-onset diabetes of the young, cAMP signaling pathway, non-alcoholic fatty liver disease, Alzheimer's disease and glycosaminoglycan biosynthesis (Fig. 1D). Compared to the GAC enrichment pattern, the GNEC patient samples displayed specific nerve cell and endocrine cell

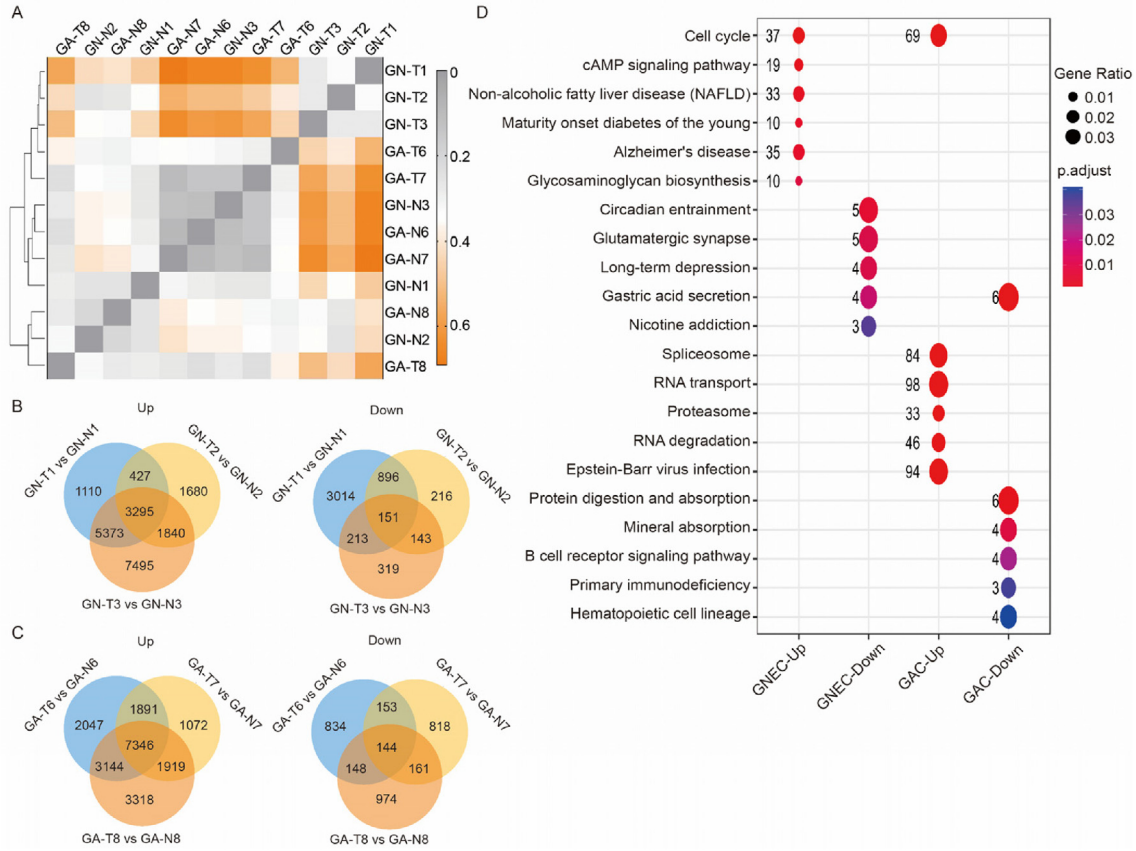

Fig. 1. Differential expression analysis and function enrichment of GNEC and GAC. (A) Gene expression distance cluster analysis between patient samples (GN-N: GNEC non-tumor tissue, GN-T: GNEC tumor tissue, GA-N: GAC non-tumor tissue, GA-T: GAC tumor tissue). (B) Venn diagram to illustrate the overlapped DEGs between GNEC samples. (C) Venn diagram to illustrate the overlapped DEGs between GAC samples. (D) The functional enrichment of GNEC and GAC specific dysregulated genes was identified in the KEGG analysis.

related disease characteristics (maturity onset diabetes of the young and Alzheimers disease). Still, they shared similar disturbance of cell cycle (Fig. 1D).

Meanwhile, we noticed the gene function enrichment pattern of downregulated genes in GNEC and GAC patient samples were significantly different. The specific downregulated genes in GNEC patient samples were mainly enriched circadian entrainment, glutamatergic synapse, long-term depression, gastric acid secretion and nicotine addiction (Fig. 1D). Noticeably, we found the abnormal of gastric acid secretion related pathway was in the downregulated gene enrichment pattern. It had been pointed out that disorder of gastric acid could lead to GNEC in mice model [17], supporting the validity of our screen.

3.2. Validation of GNEC cell lines and drug sensitivity

To the best of our knowledge, ECC10 and ECC12 were the only two GNEC cell lines available. From our current observation of these two cell lines, we noticed that both cell lines are in small cell type, and grow in grape-like clusters – "formation of cell clump" (Fig. 2A). Therefore, to confirm the reliability of these two cell lines, we first detected the levels of the two GNEC diagnosis makers CgA and SYN in ECC10 and ECC12. In comparison to GAC cell lines MGC-803 and AGS, the mRNA levels (Fig. 2B) and protein levels (Fig. 2C) of CgA and SYN were significantly higher in ECC10 and ECC12, assuring the validity of these two cell lines for further study. Firstly, the fold change of the top 6 DEGs from the above RNA-seq analyses was selected for expression detection in two GNEC and seven GAC cell lines. And we found that the expression patterns of these targets were correlated with the transcriptome results of GNEC and GAC tumor samples (Fig. 2D-2I). Next, the RNA levels of 42 DEGs (26 up-regulated gene and 16 down-regulated genes) with the most significant fold changes which were listed after the above 6 targets had been chosen for further validation in GNEC and GAC cell lines. The GNEC cell lines did demonstrate a similar unique gene expression pattern as GNEC patient tissue samples (Appendix Figs. S1 and S2), further confirming the validity of these two GNEC cell lines. Then in GAC (AGS and MGC-803) and GNEC (ECC10 and ECC12) cell lines, we tested the efficacy of chemotherapy drugs commonly used for GNEC patients including 5-fluorouracil, oxaliplatin, cisplatin and irinotecan. The two GNEC cell lines displayed lower sensitivity to chemotherapy drugs than the two GAC cell lines (Fig. 2J, K, L and M), which is consistent with our hypothesis as mentioned earlier that GNEC is more resistant to chemotherapy drugs.

3.3. Transcriptome analysis of GNEC cell lines

Considering the mixture of cancer cells with other types of cell such as connective tissues, infiltrated T cells, fibroblasts etc. in patient samples, we performed another RNA-seq using the two GNEC cell lines and two GAC cell lines AGS and MGC-803 to explore further the potential chemoresistance-related pathways and specific therapeutic targets for GNEC treatment. In total, there were 2252 up-regulated genes, and 1050 downregulated specific genes in GNEC cell lines (Fig. 3A). Compared with AGS and MGC-803, ECC10 and ECC12 contained similar gene expression pattern (Fig. 3B). The KEGG enrichment analysis showed the up-regulated genes were significantly enriched in neuroactive signaling and synapse-related pathways (Fig. 3C and D), implying that GNEC cell lines contained neuron-like characteristics.

To further narrow down the list of GNEC specific DEGs, we compared GNEC patient sample specific DEGs (GNEC versus GAC patient samples) with GNEC cell line specific DEGs (GNEC versus GAC cell lines). In total, 304 genes were overlapped (Fig. 4A), and KEGG analysis showed the overlapped genes were enriched in maturity onset diabetes of the young, proximal tubule bicarbonate reclamation, cAMP signaling pathway and MAPK signaling pathway (Fig. 4B). These four pathways contain 22 key dysregulated genes out of the 304 genes (Fig. 4C). As expected, these key genes in the respective enriched pathway clearly differentiate GNEC and GNEC cell lines from GAC, their adjacent non-tumor tissues and GAC cell lines (Fig. 1D). Notably, we found the fold change of NeuroD1 level was the most consistent in the GNEC tumor samples and GNEC cell lines, compared with their adjacent tissue samples, GAC samples and GAC cell lines. In further protein–protein interaction analysis, we found that as an important target in maturity onset diabetes of the young pathway, NeuroD1 also associated with CACNA1A enriched in MAPK signaling pathway (Fig. 5). Therefore, we speculated that NeuroD1 might be the most valuable target for further investigation.

Interestingly, it has been pointed out that in the SN38 (irinotecan metabolite) resistant HCT116 cell line, CACNA1A served as the core node in multiple differential genes and signal pathways network, and was likely to mediate irinotecan resistance [18]. Moreover, initial statistical analysis of psychotropic drug effect had shown that the changes of single nucleotide polymorphisms in CACNA1A and CACNA1H had a significant correlation with drug resistance [19]. We indicated that these genes in this network are likely to be involved in the resistance process of GNEC. Therefore, we selected NeuroD1 as a representative candidate for this network to verify whether maturity onset diabetes of the young pathway or the whole network may affect the chemoresistance.

3.4. Knockdown of NeuroD1 accelerated the growth and enhanced the sensitivity to irinotecan of GNEC cell lines

To evaluate the prognostic roles of NeuroD1 in GNEC, we performed IHC staining of NeuroD1 in 50 pairs of GNEC patient samples which were collected by our group collected over the past 10 years. In a representative MANEC patient sample, the GNEC clearly contained higher NeuroD1 protein level compared to GAC or the non-tumor tissues (Fig. 6A). According to the expression level of NeuroD1 we defined (Fig. 6B), we found the patients with lower NeuroD1 level had more prolonged survival (Fig. 6C). It suggested that NeuroD1 may be an important oncogene for GNEC, and more markers may exist in our gene panel. It was worth noting that when we used GEPIA database [20] and the Kaplan–Meier plotter database [21] to characterize the association between NeuroD1 expression and prognosis of GAC, we found that in the GEPIA cohort, the expression of NeuroD1 was not associated with overall survival of GAC patients (Fig. 6D). Exploration in the Kaplan–Meier plotter cohort of GAC patients showed similar results that the expression of NeuroD1 was not associated with overall survival of GAC patients (Fig. 6E). These results indicated that as a specific target in GNEC , NeuroD1 possesses significant and specific prognostic value for GNEC but not GAC.

In order to study the functional role of NeuroD1, we stably knocked down NeuroD1 in GNEC cell lines ECC12 and ECC10 (Fig. 6F and 6G). Based on the cell viability test within four chemotherapy drugs that we mentioned in Fig. 2J–2M, we found that under irinotecan treatment, the cell viability of GNEC NeuroD1 knockdown cell lines were significantly lower than the scramble group respectively (Fig. 6H and 6I). It indicated that NeuroD1 knockdown enhanced the sensitivity of GNEC cell lines to irinotecan, suggesting the oncogenic function of NeuroD1 may mainly contribute to the chemoresistance of GNEC cells.

4. Discussion

To the best of our knowledge, this is the first systematic transcriptome analysis of GNEC and a serial of dysregulated targets

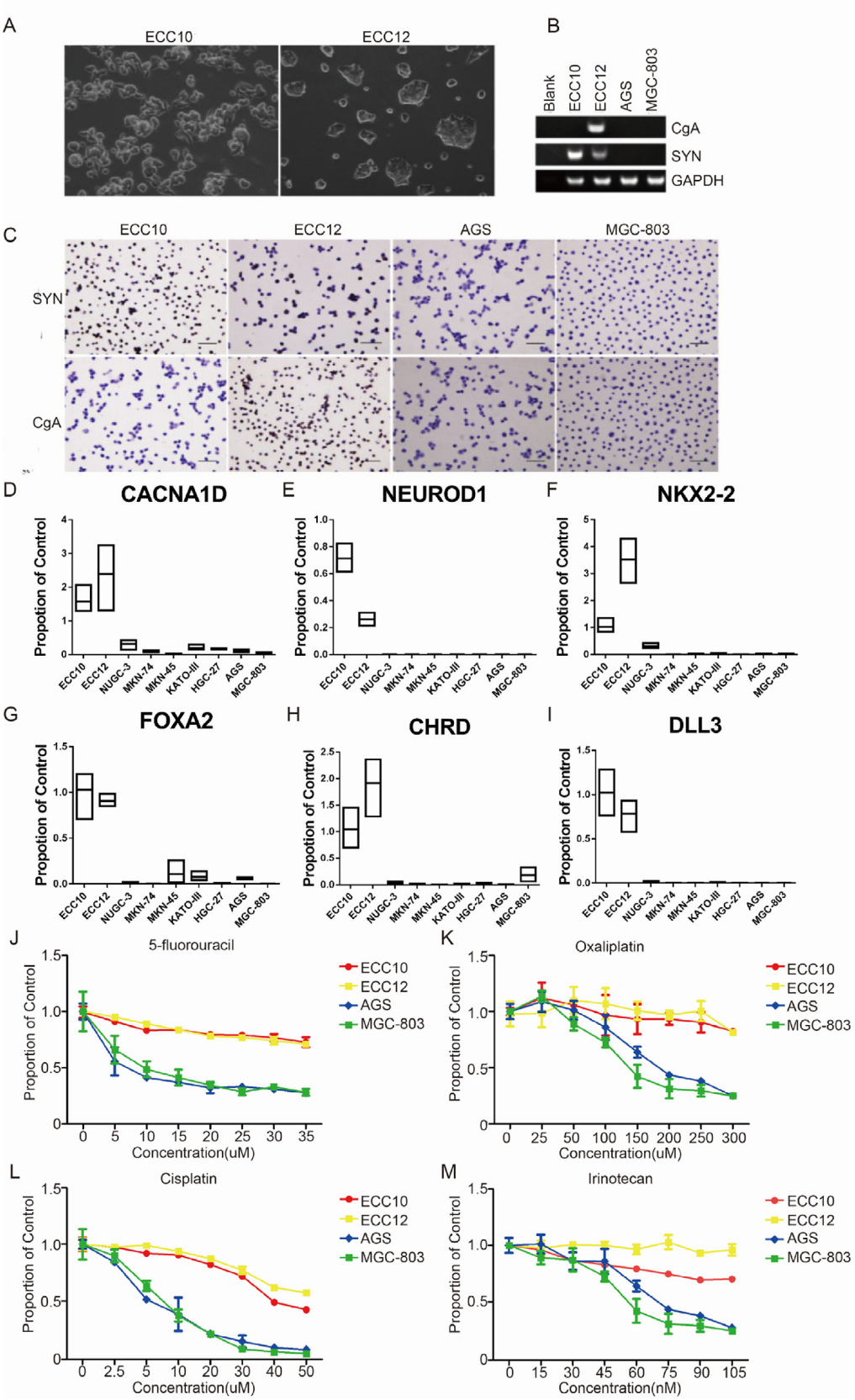

Fig. 2. GNEC cell lines verification and drug sensitivity detection. (A) ECC10 and ECC12 live cell image. (B) CgA and SYN transcriptional level detection in ECC10 and ECC12 by PCR. (C) CgA and SYN transcriptional level detection in ECC10 and ECC12 by IHC. (D-I) Validation of RNA-Seq data by quantitative PCR showed 6 selected genes in fold change top 48. (J-K) Common chemotherapy agents were tested in GNEC and GAC cell lines. Compared to GAC cell lines AGS and MGC-803, GNEC cell lines ECC10 and ECC12 have lower sensitivity to 5-fluorouracil, oxaliplatin, cisplatin and irinotecan treatment.

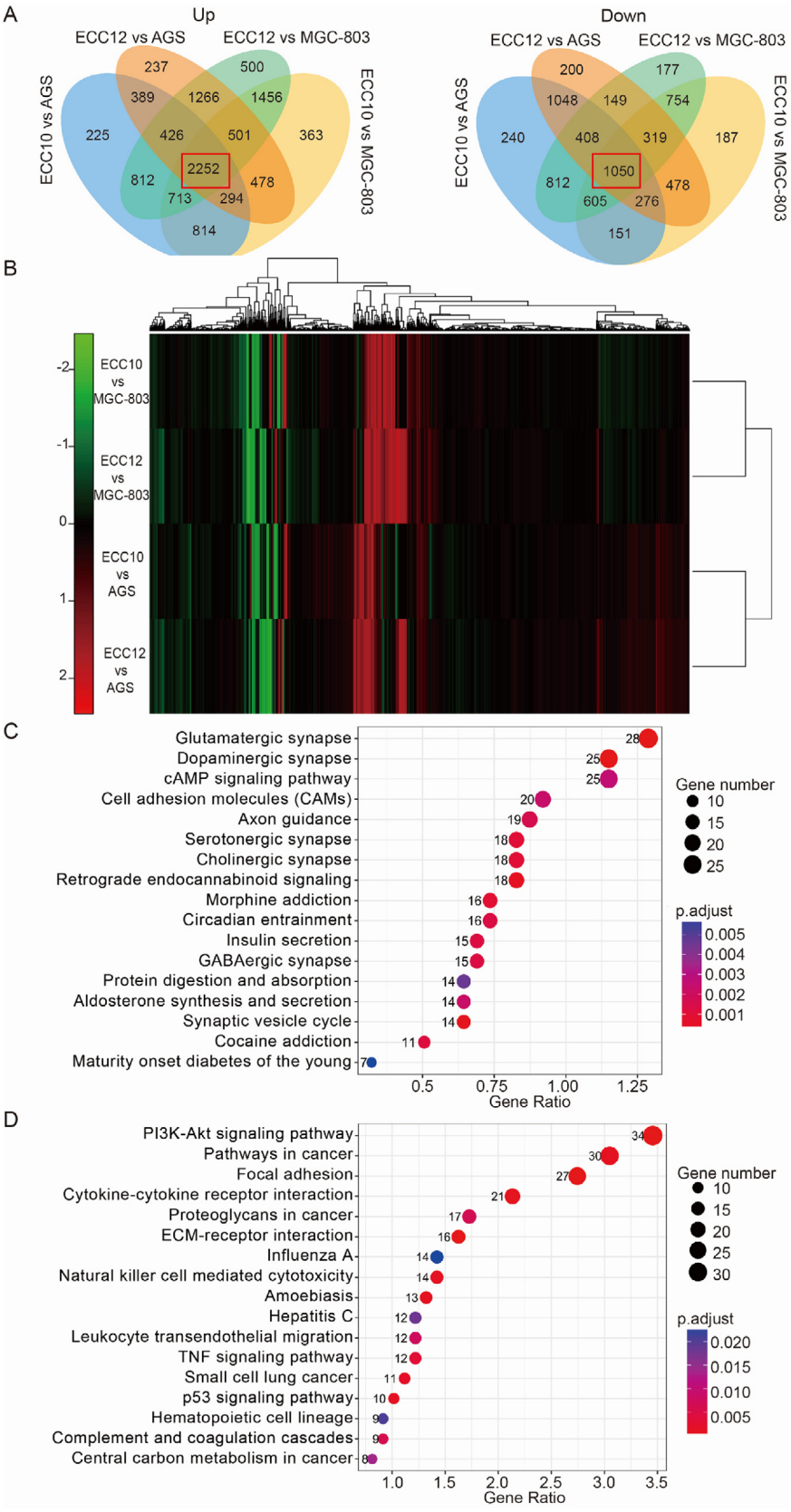

Fig. 3. Differential expression analysis and function enrichment of GNEC and GAC cell lines. (A) Venn diagram to illustrate the overlapped DEGs among the comparison of ECC10, ECC12, AGS and MGC-803. (B) Gene expression pattern among the comparison of ECC10, ECC12, AGS and MGC-803. (C) The functional enrichment of GNEC cell lines specific up dysregulated genes were identified in the KEGG analysis. (D) The functional enrichment of GNEC cell lines specific down dysregulated genes were identified in the KEGG analysis.

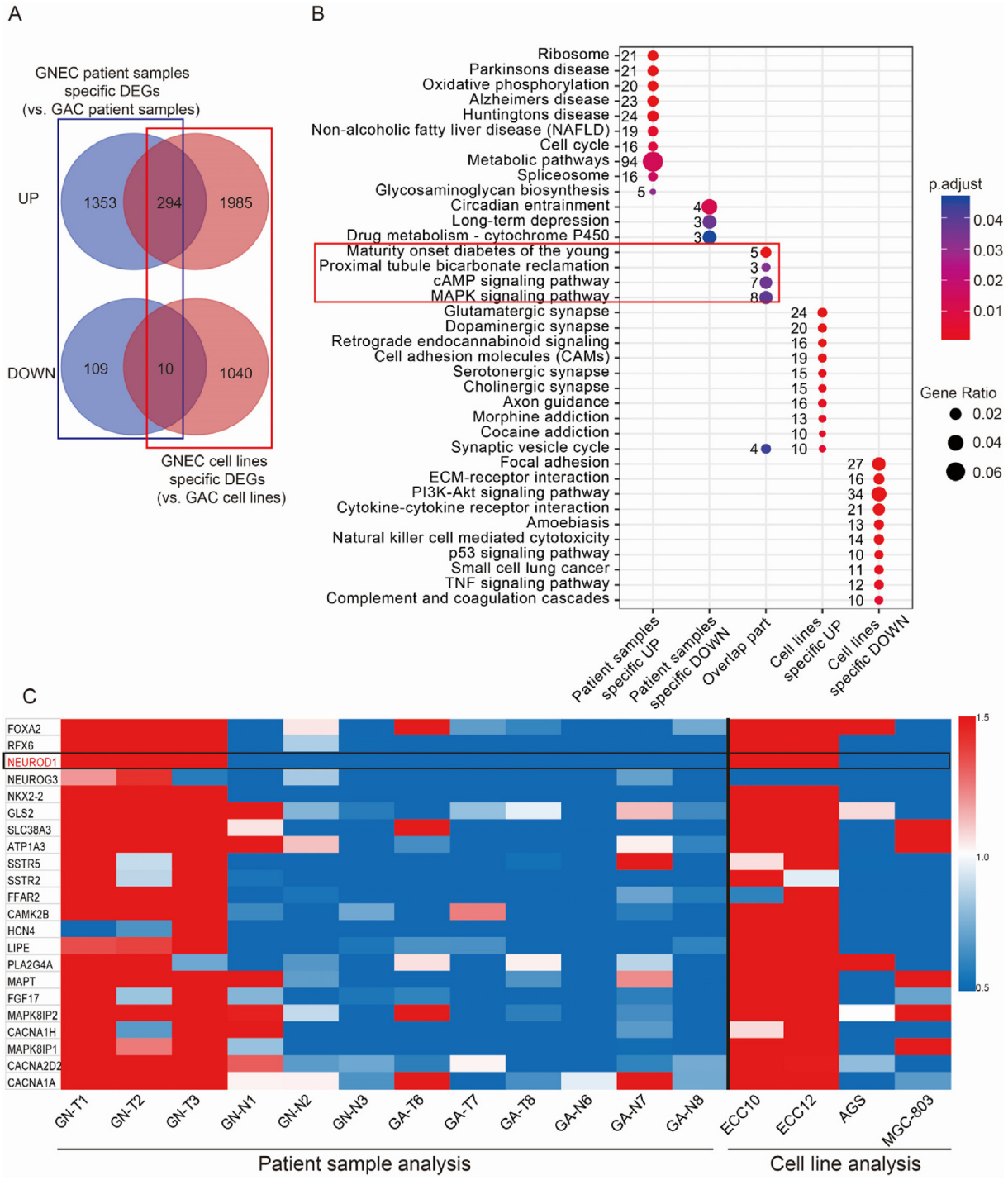

Fig. 4. Differential expression analysis and function enrichment of the comparison of patient samples and cell lines. (A) Venn diagram to illustrate the GNEC patient sample special DEGs (vs. GAC patient samples DEGs) and GNEC cell lines special DEGs (vs. GAC cell lines DEGs). (B) The functional enrichment of GNEC patient samples and cell lines specific DEGs was identified in the KEGG analysis. (C) Heatmaps showed Z scores (interpreted as a measure of SD away from the mean) of some selected genes from GNEC RNA-Seq data. The color scheme was based on the Z scores, red represents up-regulated genes, blue represents downregulated genes and gray represents undetermined directionality. (For interpretation of the references to color in this figure legend, the reader is referred to the web version of this article.)

were identified. However, there are several limitations to this study. First, due to the rarity of GNEC, only three pairs of GNEC patient samples were finally included for RNA-seq in this study due to the low GNEC incidence, which may not represent all the characteristics of GNEC. Second, although we have a frozen GNEC sample set of over 50 patient samples for IHC and the prognosis evaluation, all samples were collected in our hospital, and the number is not very big, thus reducing the reliability of the prognosis analysis. It will be ideal for accumulating more GNEC patient samples to generate a more detailed dataset of GNEC. But we feel it is more important to share the discoveries of this first GNEC transcriptome analysis to promote more interest and researches in this disease.

From RNA-seq analysis, we noticed that there were 3446 co-dysregulated genes in the comparison of the three pairs of GNEC patient sample. We found 2423 genes with protein products, 469

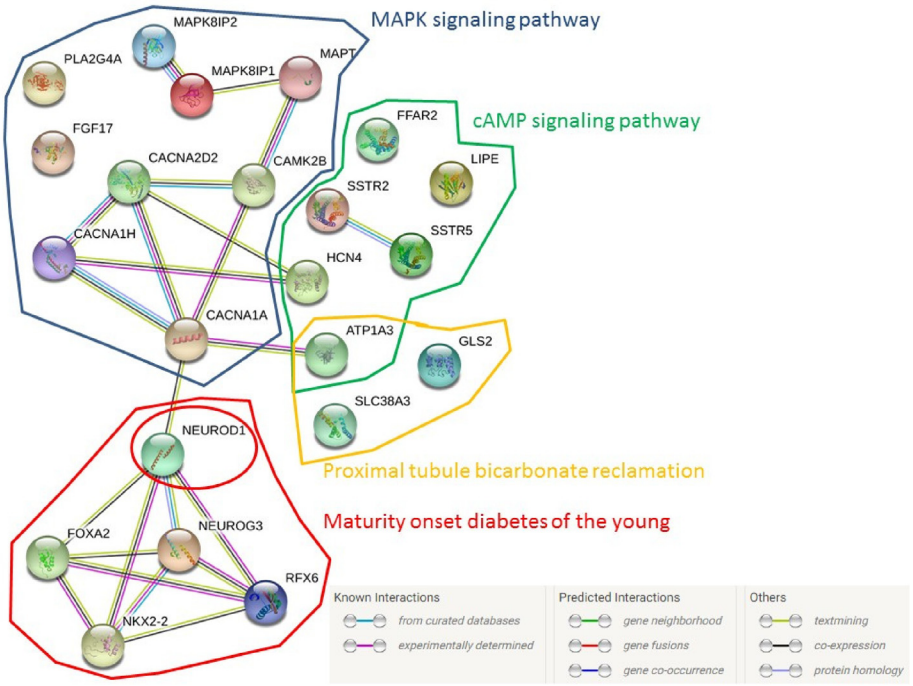

Fig. 5. Protein-protein interaction within 22 key dyregulated targets. The analysis was performed by String (https://string-db.org) within these 22 key dyregulated targets which were enriched in the four specific pathways of overlap part in the Fig. 4A (Each of the colors represents a pathway).

unknown genes and 148 non-coding RNAs. The consistency between GNEC patient tumor samples is very strong (Fig. 1A). Notably, compared with GAC, the related KEGG analysis have shown specific gene function enrichment in GNEC DEGs. Previous reports indicated that cAMP signaling promotes DNA damage repair [9] and allows cancer cells to acquire a novel mechanism that prevents the toxicity of DNA damaging agents [10,11]. Additionally, the cell cycle is strongly correlated with chemoresistance and DNA damage repair [12,13]. The enrichment of cAMP and the cell cycle pathway in GNEC may be one of the reasons why GNEC patients are more resistant to DNA alkylating agents that lead to poorer survival.

Based on the significant prognosis difference between GNEC and GAC, these differential genes may answer the existing chemoresistance state in GNEC clinical treatment and offer emerging targets for optimizing GNEC specific chemotherapy strategy. However, it is hard to avoid that sampling deviation, and potential immune cell infiltration would affect the accuracy of DEGs result and further target selection. In order to find out the difference between GNEC and GAC, we compared GNEC and GAC patient sample RNA-seq with cell line RNA-seq data, which can help ulteriorly eliminate the nonspecific DEGs from GNEC patient samples. Finally, in total, 304 DEGs became our focus. From the KEGG analysis within these DEGs, we noticed that maturity onset diabetes of the young, proximal tubule bicarbonate reclamation, cAMP signaling pathway and MAPK signaling pathway were specifically dysregulated in GNEC, and maturity onset diabetes of the young pathway was the most significant one. In further PPI analysis, we explored the interrelationships among the 22 genes which were enriched in these four specific pathways (Fig. 5). Based on protein correlations, we found that compared to proximal tubule bicarbonate reclamation and cAMP signaling pathway, the gene correlation in maturity onset diabetes of the young pathway and MAPK signaling pathway was closer.

From this PPI analysis, we found that NeuroD1 and CACNA1A had co-expression relationship. It had been reported that knockout of NeuroD1 in murine β-Cell would downregulate the expression level of CACNA1A [22]. As an essential neuron development related transcription factor, NeuroD1 is involved in regulating the insulin secretory process [22]. At the same time, some researches had pointed out that it was involved in the development of small cell lung cancer (SCLC) and neuroblastoma [23,24]. Also, we noticed that in estrogen receptor-negative breast cancers, high NeuroD1 methylation was more likely to respond with a complete pathologic response following neoadjuvant chemotherapy [25]. Considering the potential value of maturity onset diabetes of the young pathway and roles of NeuroD1 in neuron development and some NETs, we chose NeuroD1 as a candidate to verify the GNEC chemoresistance. When we disturbed NeuroD1 expression, the GNEC cells became more sensitive to irinotecan. In the future, the related *in vivo* experiments would be performed to validate the changes of chemosensitivity using GNEC cell line xenograft model.

Meanwhile, in maturity onset diabetes of the young pathway, absence of NKX2.2 in primary tumor samples of small cell lung cancer was an independent predictor of improved outcomes in chemotherapy-treated patients [26]. In the MAPK signaling pathway, in addition to the related resistance studies of CACNA1A mentioned in the result section, we also noticed in osteosarcoma, knockdown MAPK8IP1 would enhance the efficacy of doxorubicin treatment [27]. Moreover, as an important protein in the MAPK signaling pathway, microtubule-associated protein tau (MAPT) was involved in cisplatin and paclitaxel resistance mechanisms in gastric cancer, non-small cell lung cancer, and ovarian cancer [28–30]. Based on KEGG analysis within GNEC specific DEGs and related drug resistance studies, we speculate that these 22 genes included in these four specifically enriched pathways may be important regulatory factors in the resistance mechanism of GNEC chemotherapy.

Therefore, we had a reason to believe that this specific panel in GNEC gene expression pattern was involved in the mechanism of GNEC chemotherapy drug tolerance. Subsequent research on this

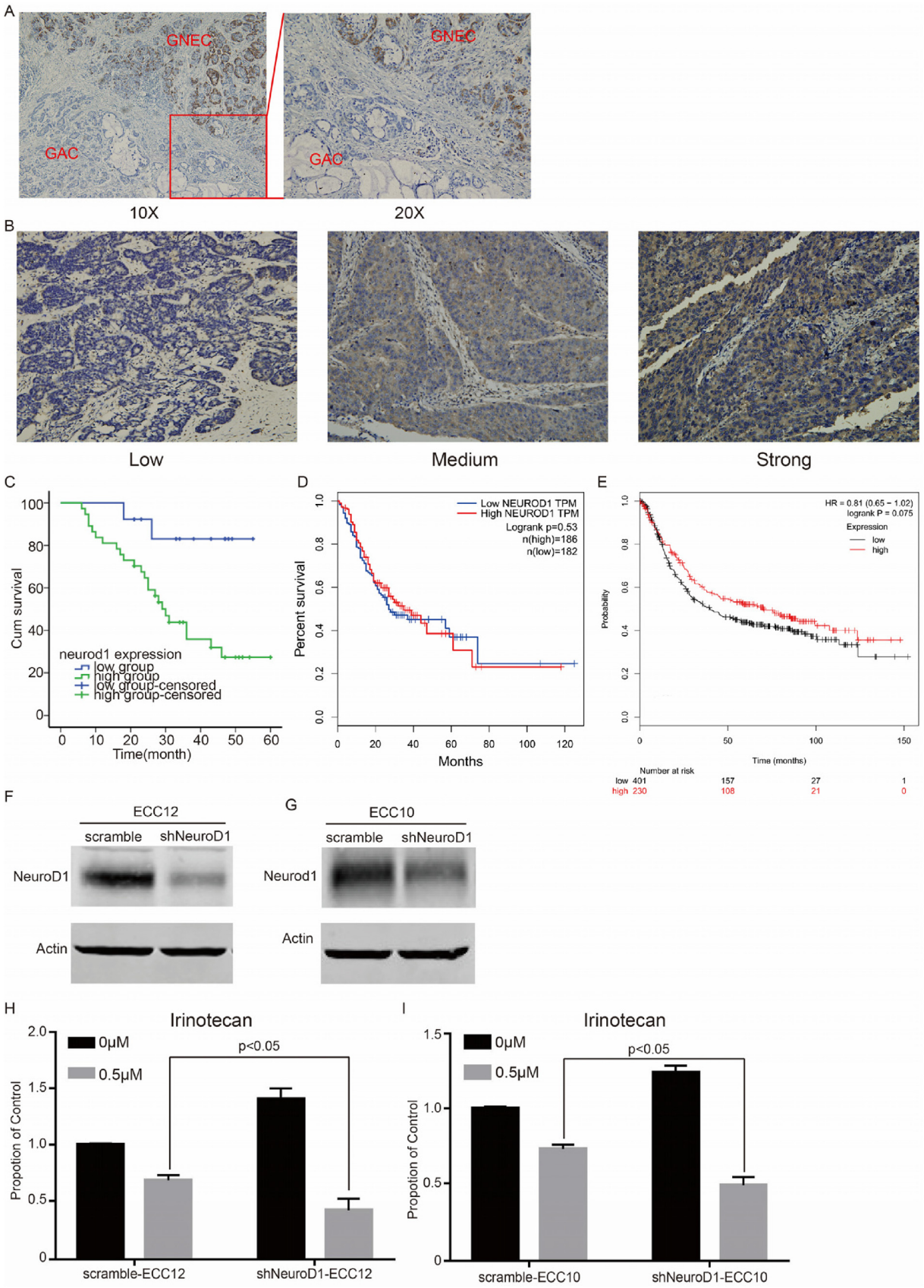

Fig. 6. Evaluation of the prognostic and chemoresisitance roles of NeuroD1 in GNEC. (A) NeuroD1immunohistochemical verification in MANECs. Compared to GAC part, GNEC part contained high expression level. The top image with 20X magnification is the amplification of the red outlined part in bottom image. (B) Criteria for the degree of gene expression in immunohistochemical experiment. (C) Comparison of overall survival curves for NeuroD1 low and high expression group in GNEC patients. The expression of NeuroD1 was not correlated with overall survival in the GEPIA cohort (D) and the Kaplan–Meier plotter cohort (E). (F and G) The knockdown effect of NeuoD1 in GNEC cell lines. (H and I) Knock down NeuroD1 promoted chemosensitivity of GNEC cell lines to irinotecan (cell viability test), data are presented as mean ± SEM. (For interpretation of the references to color in this figure legend, the reader is referred to the web version of this article.)

signal pathway will provide a theoretical basis for GNEC to discover specific chemoresistance mechanisms and chemotherapy strategies.

5. Conclusions

Compared to the GAC enrichment pattern, the GNEC patient samples displayed specific nerve cell and endocrine cell related disease characteristics (maturity onset diabetes of the young and Alzheimer's disease), which GNEC showed significant difference with GAC patient samples. Moreover, cAMP signaling and cell cycle related pathway existed in KEGG enrichment suggested that GNEC may contain high DNA damage repair ability and chemoresistance. Further chemosensitivity detection experiment *in vitro* showed GNEC cell lines ECC10 and ECC12 displayed significant chemoresistance ability, compared with GAC cell lines AGS and MGC-803. Through more RNA-seq analysis, we found the co-regulated genes from the DEGs of patient samples and cell lines were enriched in maturity onset diabetes of the young, proximal tubule bicarbonate reclamation, cAMP signaling pathway and MAPK signaling pathway. In further exploration, the IHC results indicated that NeuroD1 possesses significant prognosis value for GNEC but not GAC. Then we found that knockdown of NeuroD1 enhanced the sensitivity of GNEC cell lines to irinotecan, suggesting the abnormal of these GNEC specific DEGs enriched in these four pathways may contribute to the chemoresistance of GNEC cells.

Declaration of Competing Interest

The authors declare that they have no known competing financial interests or personal relationships that could have appeared to influence the work reported in this paper.

Acknowledgements

The authors would like to thank the Fujian Medical University Union Hospital, the College of Life Sciences in Fujian Normal University and the Genomics, Bioinformatics & Single Cell Analysis Core at the Faculty of Health Sciences University of Macau for providing experimental equipment and technical support.

Authors' contributions

CH, HFK and YL designed the study. JX, PC, HX, YS, ZH, KHW, ZM, SDZ, and QW performed experiments and participated in analyses of data; PC, HX and RW performed manuscript drafting. CH, HFK and YL revised the manuscript. All authors read and approved the final manuscript.

Ethics approval and consent to participate

The study was approved by the ethics committee of Fujian Medical University Union Hospital (Fujian, China; 2017KY090). Human tissue specimens collected for this study were from residual tissue in blocks generated for gastrectomy processing. All patients signed informed consents agreeing on further examinations and investigations.

Data availability

All data and materials generated during and/or analysed during the current study are available from the corresponding author on reasonable request.

Funding information

This work was supported by National Natural Science Foundation of China (No. 81871899), the International S&T Cooperation Program of China (2016YFE0121900), the Scientific Research Innovation Team Construction Program of Fujian Normal University (IRTL1702), the United Fujian Provincial Health & Education Project for Tackling the Key Research (WKJ2016-2-27), the Natural Science Foundation of Fujian Province (2016Y0029), the Science and Technology Development Fund, Macau SAR (File no. 0055/2019/A1), the Scientific and Technological Innovation Joint Capital Projects of Fujian Province (2016Y9031), the National Key Clinical Specialty Discipline Construction Program of China (No. [2012]649), the Chinese Society of Clinical Oncology (Y-N2014-008), and the Medical Innovation Projects of Fujian Province (2015-CXB-16).

Appendix A. Supplementary data

Supplementary data to this article can be found online at https://doi.org/10.1016/j.csbj.2020.09.016.

References

[1] Modlin IM, Lye KD, Kidd M. Carcinoid tumors of the stomach. Surg Oncol 2003;12(2):153–72.
[2] Yao JC, Hassan M, Phan A, Dagohoy C, Leary C, et al. One hundred years after "carcinoid": epidemiology of and prognostic factors for neuroendocrine tumors in 35,825 cases in the United States. J Clin Oncol 2008;26(18):3063–72.
[3] Ito T, Igarashi H, Nakamura K, Sasano H, Okusaka T, Takano K, Komoto I, Tanaka M, Imamura M, Jensen RT, Takayanagi R, Shimatsu A. Epidemiological trends of pancreatic and gastrointestinal neuroendocrine tumors in Japan: a nationwide survey analysis. J Gastroenterol 2015;50(1):58–64.
[4] Cao LL, Lu J, Lin JX, Zheng CH, Li P et al., (2016) A novel predictive model based on preoperative blood neutrophil-to-lymphocyte ratio for survival prognosis in patients with gastric neuroendocrine neoplasms. Oncotarget 7 (27), 42045-58.
[5] Hadoux J, Malka D, Planchard D, Scoazec JY, Caramella C et al., (2015) Post-first-line FOLFOX chemotherapy for grade 3 neuroendocrine carcinoma. Endocrine-related cancer 22 (3), 289-98.
[6] Bajetta E, Catena L, Biondani P, Pusceddu S, Valente M, et al. Activity of a three-drug combination including cisplatin (CLOVER regimen) for poorly differentiated neuroendocrine carcinoma. Anticancer Res 2014;34 (10):5657–60.
[7] Xie J-W, Lu J, Lin J-X, Zheng C-H, Li P, Wang J-B, Chen Q-Y, Cao L-L, Lin Mi, Tu R-H, Huang C-M. Different long-term oncologic outcomes after radical surgical resection for neuroendocrine carcinoma and adenocarcinoma of the stomach. Oncotarget 2017;8(34):57495–504.
[8] Acosta AM, Wiley EL, (2016) Primary Biliary Mixed Adenoneuroendocrine Carcinoma (MANEC): A Short Review. Archives of pathology & laboratory medicine 140 (10), 1157-62.
[9] Jarrett SG, Wolf Horrell EM, D'Orazio JA, (2016) AKAP12 mediates PKA-induced phosphorylation of ATR to enhance nucleotide excision repair. Nucleic acids research 44 (22), 10711-26.
[10] Jarrett SG, Carter KM, Shelton BJ, D'Orazio JA. The melanocortin signaling cAMP axis accelerates repair and reduces mutagenesis of platinum-induced DNA damage. Sci Rep 2017;7(1):11708.
[11] Xiao L-Y, Kan W-M. Cyclic AMP (cAMP) confers drug resistance against DNA damaging agents via PKAIA in CML cells. Eur J Pharmacol 2017;794:201–8.
[12] Hasan S, Taha R, Omri HE. Current opinions on chemoresistance: an overview. Bioinformation 2018;14(02):80–5.
[13] Pérez-Yépez EA, Saldívar-Cerón HI, Villamar-Cruz O, Pérez-Plasencia C, Arias-Romero LE. p21 Activated kinase 1: Nuclear activity and its role during DNA damage repair. DNA Repair 2018;65:42–6.
[14] Öberg K, Kvols L, Caplin M, Delle Fave G, de Herder W, Rindi G, Ruszniewski P, Woltering EA, Wiedenmann B. Consensus report on the use of somatostatin analogs for the management of neuroendocrine tumors of the gastroenteropancreatic system. Ann Oncol 2004;15(6):966–73.
[15] Sun Y-Q, Xie J-W, Xie H-T, Chen P-C, Zhang X-L, Zheng C-H, Li P, Wang J-B, Lin J-X, Cao L-L, Huang C-M, Lin Y. Expression of CRM1 and CDK5 shows high prognostic accuracy for gastric cancer. World J Gastroenterol 2017;23 (11):2012.
[16] Lu J, Lin JX, Zhang PY, Sun YQ, Li P, et al. CDK5 suppresses the metastasis of gastric cancer cells by interacting with and regulating PP2A. Oncol Rep 2019;41(2):779–88.
[17] Calvete O, Varro A, Pritchard DM, Barroso A, Oteo M, Morcillo MÁ, Vargiu P, Dodd S, Garcia M, Reyes J, Ortega S, Benitez J. A knockin mouse model for human ATP4a R703C mutation identified in familial gastric neuroendocrine tumors recapitulates the premalignant condition of the human disease and suggests new therapeutic strategies. Dis Model Mech 2016;9(9):975–84.

[18] Zheng Y, Zhou J, Tong Y. Gene signatures of drug resistance predict patient survival in colorectal cancer. Pharmacogenomics J 2015;15(2):135–43.
[19] Lv N, Qu J, Long H, Zhou L, Cao Y, Long L, Liu Z, Xiao Bo. Association study between polymorphisms in the CACNA1A, CACNA1C, and CACNA1H genes and drug-resistant epilepsy in the Chinese Han population. Seizure 2015;30:64–9.
[20] Tang Z, Li C, Kang B, Gao G, Li C et al., (2017) GEPIA: a web server for cancer and normal gene expression profiling and interactive analyses. Nucleic acids research 45 (W1), W98-W102.
[21] Szász AM, Lánczky A, Nagy Á, Förster S, Hark K, Green JE, Boussioutas A, Busuttil R, Szabó A, Győrffy B. Cross-validation of survival associated biomarkers in gastric cancer using transcriptomic data of 1,065 patients. Oncotarget 2016;7(31):49322–33.
[22] Romer AI, Singer RA, Sui L, Egli D, Sussel L. Murine perinatal beta-cell proliferation and the differentiation of human stem cell-derived insulin-expressing cells require NEUROD1. Diabetes 2019;68(12):2259–71.
[23] Borromeo M, Savage T, Kollipara R, He M, Augustyn A, Osborne J, Girard L, Minna J, Gazdar A, Cobb M, Johnson J. ASCL1 and NEUROD1 reveal heterogeneity in pulmonary neuroendocrine tumors and regulate distinct genetic programs. Cell Reports 2016;16(5):1259–72.
[24] Lu F, Kishida S, Mu P, Huang P, Cao D, Tsubota S, Kadomatsu K. NeuroD1 promotes neuroblastoma cell growth by inducing the expression of ALK. Cancer Sci 2015;106(4):390–6.
[25] Fiegl H, Jones A, Hauser-Kronberger C, Hutarew G, Reitsamer R, Jones RL, Dowsett M, Mueller-Holzner E, Windbichler G, Daxenbichler G, Goebel G, Ensinger C, Jacobs I, Widschwendter M. Methylated NEUROD1 promoter is a marker for chemosensitivity in breast cancer. Clin Cancer Res 2008;14 (11):3494–502.
[26] Lawson MH, Cummings NM, Rassl DM, Russell R, Brenton JD, Rintoul RC, Murphy G. Two novel determinants of etoposide resistance in small cell lung cancer. Cancer Res 2011;71(14):4877–87.
[27] Posthuma De Boer J, van Egmond PW, Helder MN, de Menezes RX, Cleton-Jansen A-M, Beliën JAM, Verheul HMW, van Royen BJ, Kaspers G-J, van Beusechem VW. Targeting JNK-interacting protein 1 (JIP1) sensitises osteosarcoma to doxorubicin. Oncotarget 2012;3(10):1169–81.
[28] Wu H, Huang M, Lu M, Zhu W, Shu Y, Cao P, Liu P. Regulation of microtubule-associated protein tau (MAPT) by miR-34c-5p determines the chemosensitivity of gastric cancer to paclitaxel. Cancer Chemother Pharmacol 2013;71(5):1159–71.
[29] Ribeiro JR, Schorl C, Yano N, Romano N, Kim KK, Singh RK, Moore RG. HE4 promotes collateral resistance to cisplatin and paclitaxel in ovarian cancer cells. J Ovarian Res 2016;9(1).
[30] Ye J, Zhang Z, Sun L, Fang Y, Xu X, Zhou G. miR-186 regulates chemo-sensitivity to paclitaxel via targeting MAPT in non-small cell lung cancer (NSCLC). Mol BioSyst 2016;12(11):3417–24.